

Spectra and cycle structure of trophically coherent graphs

Samuel Johnson^{1*} and Nick S. Jones²

¹Warwick Mathematics Institute, and Centre for Complexity Science,
University of Warwick, Coventry CV4 7AL, United Kingdom.

²Department of Mathematics, Imperial College London,
London SW7 2AZ, United Kingdom.

*E-mail: S.Johnson.2@warwick.ac.uk

Abstract

Many natural, complex systems are remarkably stable thanks to an absence of feedback acting on their elements. When described as networks, these exhibit few or no cycles and have small leading eigenvalues. It has been suggested that this architecture can confer advantages to the system as a whole, but this observation does not in itself explain how a ‘loop-less’ structure might arise. We show here that feedback loops and leading eigenvalues are suppressed by a structural property called trophic coherence, which was recently shown to account for the stability of food webs. Our theory correctly classifies a variety of networks – including those of genes, metabolites, species, neurons, words, computers and trading nations – into two distinct regimes of high and low feedback, and provides a null-model to gauge the significance of related magnitudes. These findings suggest a parsimonious explanation for the existence of ‘qualitative stability’ in nature, and show that network trophic structure can illuminate important characteristics of many complex systems.

Introduction

Feedback is a fundamental process in dynamical systems which occurs when the output of an element is coupled to its input. In complex systems, this coupling can happen via feedback loops (or cycles) involving many elements, and hence the number and structure of such loops often determine important properties of the system as a whole [1]. In systems which can be represented as graphs, or networks, the combined effects of feedback loops are described by the spectrum of eigenvalues of the adjacency matrix (the matrix of ones and zeros representing the existence or absence of edges between nodes) [2, 3]. These eigenvalues can be related to fundamental questions regarding both structure [4, 5] and dynamical processes – including percolation [6], stability of dynamical elements [7], diffusion [8], or synchronization of coupled oscillators [2].

It has been observed that many biological networks, such as food webs [9] and gene transcription networks [10], have far fewer feedback loops than would be randomly expected, or even none at all. Given that acyclicity is the main

requirement for being ‘qualitatively stable’, or stable regardless of the details of dynamics [1], one might suppose that this ‘loopless’ architecture is an adaptation for stability or some other functional advantage. However, in some cases it is not clear what the optimisation mechanism behind loop suppression might be. In an ecosystem, for instance, how would a feedback cycle be eliminated if it happened to benefit the particular organisms involved?

It has recently been shown that the high linear stability of food webs is determined mainly by a structural feature called ‘trophic coherence’, a measure of how neatly nodes fall into distinct levels [11]. Trophic coherence, moreover, has been found to play an important role in other structural and dynamical properties of networks [12, 13]. In order to investigate the relationship between trophic coherence and feedback, we here define the ‘coherence ensemble’ of graphs, and obtain expressions for various magnitudes relating to the cycle structure and spectrum of eigenvalues of coherent but otherwise random networks. We find that the key ingredient is a parameter τ which determines which of two regimes a given network belongs to. In one, leading eigenvalues are large and the number of directed cycles of length ν grows exponentially with ν ; in the other, all eigenvalues have real parts close to zero, and graphs have few cycles. In fact, the probability of drawing a directed acyclic graph in this regime tends to one with decreasing τ . The expectation for the leading eigenvalue, in either regime, is simply $\overline{\lambda_1} = e^\tau$. We analyse a collection of empirical networks of several kinds, and find that they conform very well to our theoretical predictions, with those networks with negative values of τ displaying very few or no cycles. In other words, the observed scarcity of feedback in certain natural systems is to be expected given their trophic coherence.

Results

Consider the directed, unweighted graph given by the $N \times N$ adjacency matrix $A = (a_{ij})$, which has $L = \sum_{ij} a_{ij}$ directed edges. The in- and out-degrees of node i are $k_i^{in} = \sum_j a_{ij}$ and $k_i^{out} = \sum_j a_{ji}$, respectively, and the mean degree is $\langle k \rangle = L/N$ (we shall use the notation $\langle \cdot \rangle$ to refer to averages over elements in a given graph, as opposed to ensemble averages). The eigenspectrum of A is $\{\lambda_i\}$. The distribution of eigenvalues, $p(\lambda)$, is related to powers of A via its moments:

$$\langle \lambda^\nu \rangle = \frac{1}{N} \text{Tr}(A^\nu). \quad (1)$$

Since A is not, in general, symmetric, its eigenvalues will be complex. The trace of A is real and invariant with respect to a change of basis, so the eigenvalues of A will always be distributed symmetrically around the real axis. Of particular interest is the eigenvalue with largest real part, λ_1 – usually referred to as A ’s leading eigenvalue.

A ‘basal node’ is one with in-degree equal to zero. If a graph has at least one basal node (our assumption throughout), and every node belongs to at least one directed path which includes a basal node, we can define the trophic level of each node i as

$$s_i = 1 + \frac{1}{k_i^{in}} \sum_j a_{ij} s_j. \quad (2)$$

With no loss of generality for subsequent results, we define the trophic level of basal nodes as $s_i = 1$, as is the convention in ecology. The ‘trophic difference’ associated to each edge is $x_{ij} = s_i - s_j$ [11]. The distribution of trophic differences $p(x)$ has mean $\langle x \rangle = 1$ by definition, and we can measure the graph’s ‘trophic coherence’ with the standard deviation

$$q = \sqrt{\langle x^2 \rangle - 1}.$$

A graph will be more trophically coherent the closer q is to zero, so we refer to q as an ‘incoherence parameter’.

The number of directed paths (henceforth ‘paths’) of length ν in A is $n_\nu = \sum_{ij} (A^\nu)_{ij}$. The number of directed cycles (henceforth ‘cycles’) of length ν is $m_\nu = \text{Tr}(A^\nu)$, which, according to Eq. (1), can be expressed as $m_\nu = N \langle \lambda^\nu \rangle$. (Note that we are not referring here to simple paths and simple cycles, in which no node can be repeated.) This definition of m_ν counts every unique cycle ν times, so the number of unique cycles will be $m_\nu^u = m_\nu / \nu$.

The directed configuration ensemble. This is the set of all graphs with given sequences of in- and out-degrees [14]. Using this ensemble as a null-model, we can obtain the expected numbers of paths and cycles by inserting the expected value of the adjacency matrix for large graphs, $\hat{a}_{ij} = k_i^{\text{out}} k_j^{\text{in}} / L$, in the above definitions (we shall use the notation \hat{z} to refer to the expected value of a magnitude z in the directed configuration ensemble). Thus, the expected number of paths in this ensemble is

$$\hat{n}_\nu = L \alpha^{\nu-1}, \quad (3)$$

while the expected number of those paths which are cycles is

$$\hat{m}_\nu = \alpha^\nu, \quad (4)$$

where

$$\alpha \equiv \frac{\langle k^{\text{in}} k^{\text{out}} \rangle}{\langle k \rangle} \quad (5)$$

captures the correlation between the in- and out-degrees of nodes (i.e. $\alpha > 1$ indicates a positive correlation, with high in-degree nodes also tending to have high out-degree, while $\alpha < 1$ means this correlation is negative).

The basal mean-field ensemble. Let us define an ensemble in which there are only two classes of nodes: B basal nodes, and $N - B$ non-basal nodes; of the L edges, L_B emanate from the basal nodes while the remaining $L - L_B$ occur between non-basal nodes. We refer to this as ‘mean field’ because all non-basal nodes are considered to have the same properties (and we shall use the notation \tilde{z} for the expected value of a magnitude z). This ensemble comprises all networks with given $\{N, B, L, L_B\}$ such that every non-basal node i with in-degree k_i^{in} receives $k_i^{\text{in}} L_B / L$ edges from basal nodes and $(1 - L_B / L) k_i^{\text{in}}$ from non-basal nodes.

We can obtain expected values for several magnitudes in this ensemble as follows. Let \tilde{s}_{nb} be the expected trophic level of a node given that it is not

basal. Since the expected proportion of in-neighbours which are basal, for such a node, will be L_B/L , we have from Eq. (2) that

$$\tilde{s}_{nb} = 1 + \frac{L_B + (L - L_B)\tilde{s}_{nb}}{L},$$

and so $\tilde{s}_{nb} = L/L_B + 1$. The mean trophic level of the network is therefore

$$\tilde{s} = 1 + \left(1 - \frac{B}{N}\right) \frac{L}{L_B}. \quad (6)$$

In the basal mean-field ensemble there will be two types of edges: those which emanate from basal nodes, with trophic difference $x = \tilde{s}_{nb} - 1$, and those between non-basal nodes, with $x = 0$. In other words, the distribution of differences will be

$$p(x) = \frac{L_B}{L} \delta\left(x - \frac{L}{L_B}\right) + \left(1 - \frac{L_B}{L}\right) \delta(x). \quad (7)$$

The trophic coherence associated with this distribution is

$$\tilde{q} = \sqrt{\frac{L}{L_B} - 1}. \quad (8)$$

We can also obtain the expected value of α in the basal mean-field ensemble. Let us consider a generic non-basal node with $k^{in} = L/(N - B)$ and $k^{out} = (L - L_B)/(N - B)$; assuming these values for all nodes with $k_{in} \neq 0$, Eq. (5) gives

$$\tilde{\alpha} = \frac{L - L_B}{N - B}. \quad (9)$$

Note that this is the mean degree that would result if all basal nodes and edges emanating from basal nodes were eliminated from the network. As in the configuration ensemble, the expected proportion of paths of length ν which are cycles, in the basal mean-field ensemble, is

$$\tilde{c}_\nu = \frac{\tilde{\alpha}}{L}. \quad (10)$$

The basal mean-field ensemble does not include any structure which might lead to variance in the trophic levels of non-basal nodes, and so the bimodal $p(x)$ given by Eq. (7) is exact. For networks in which different non-basal nodes are connected to differing proportions of basal nodes, this expression will be a valid approximation only when the separation of the two modes of $p(x)$ is much larger than the spread about them. In Supplemental Material (SM) we analyse networks generated with the directed configuration model and power-law in- and out-degree distributions, and of directed versions of Erdős-Rényi random graphs. We give numerical evidence that Eqs. (6) and (8) provide good estimates of the mean trophic level and trophic coherence, respectively, for networks in these ensembles, regardless of the heterogeneity of in- and out-degree distributions.

The coherence ensemble. Let us now consider the ensemble of graphs which not only have given in- and out-degree distributions (as in the directed configuration ensemble), but also given trophic coherence. We shall refer to this as the ‘coherence ensemble’, and use the notation $E(z) = \bar{z}$ for the expected values

of magnitudes z in this ensemble. For networks in the coherence ensemble, the probability of a randomly chosen path of length ν being a cycle can be obtained by considering a random walk along the edges of the graph and computing the probability that it returns to the initial node after ν hops. This constraint implies that the sum of the trophic differences x_k over the $k = 1, \dots, \nu$ edges involved, $S = \sum_k x_k$, must be zero. Let us approximate the differences x_k as independent random variables drawn from the trophic difference distribution $p(x)$. According to the central limit theorem, the distribution $p(S)$ will tend, with increasing ν , to a Gaussian with mean $\nu\langle x \rangle = \nu$ and variance νq^2 . Since cycles are paths which satisfy $S = 0$, the expected proportion of paths of length ν that are cycles, \bar{c}_ν , will be proportional to $p(S = 0)$. That is,

$$\bar{c}_\nu = B_\nu \frac{1}{\sqrt{\nu}q} \exp\left(-\frac{\nu}{2q^2}\right). \quad (11)$$

Not all the paths satisfying $S = 0$ will return to the initial node, and this effect is accounted for by the factor B_ν . We can obtain B_ν by particularising for the basal mean-field ensemble case, for which q and c_ν are given by Eqs. (8) and (10), respectively. Inserting these values into Eq. (11), we have

$$B_\nu = \frac{\tilde{\alpha}}{L} \sqrt{\nu} \tilde{q} \exp\left(\frac{\nu}{2\tilde{q}^2}\right).$$

Therefore, the general expression for \bar{c}_ν is

$$\bar{c}_\nu = \frac{\tilde{\alpha} \tilde{q}}{L q} \exp\left[\frac{\nu}{2} \left(\frac{1}{\tilde{q}^2} - \frac{1}{q^2}\right)\right]. \quad (12)$$

The expected proportion of paths of size ν which are cycles can thus either decrease or increase exponentially with ν , depending on whether a particular graph is more or less trophically coherent than the null expectation given its degree sequence. Eq. (12) was obtained using the central limit theorem, and so should only be valid for moderately large ν . However, if the distribution of differences, $p(x)$, is approximately normal, it will be a good approximation also at low values of ν .

Let us now assume that $\bar{n}_\nu \simeq \hat{n}_\nu$, irrespectively of q . This is a reasonable assumption, at least for low ν , since α is the key element determining the number of ways a set of edges can be concatenated. (For finite N , the approximation may break down at high ν and low q , because the maximum path length will be shorter in highly coherent graphs than in random ones.) Combining Eqs. (3) and Eq. (12) we obtain the expected number of cycles of length ν :

$$\bar{m}_\nu = \frac{\tilde{\alpha} \tilde{q}}{\alpha q} e^{\tau \nu}, \quad (13)$$

where

$$\tau = \ln \alpha + \frac{1}{2\tilde{q}^2} - \frac{1}{2q^2}. \quad (14)$$

Note that the term $1/\tilde{q}^2 - 1/q^2$ will be negative for networks which are more coherent than the random expectation ($q < \tilde{q}$), and positive for those which are less so; while the sign of $\ln \alpha$ depends on whether α is greater or smaller than 1. Eqs. (13) and (14) imply that the expected number of cycles of length

ν in a graph can either grow exponentially with ν , when $\tau > 0$; or decrease exponentially, if $\tau < 0$. Thus, which of these two regimes a given graph finds itself in is determined by the correlation between in- and out-degrees, $\alpha = \langle k^{in} k^{out} \rangle / \langle k \rangle$; the proportion of edges which connect to basal nodes, L_B/L (via $\tilde{q} = \sqrt{L/L_B - 1}$), and the trophic coherence, given by q . Note that, as mentioned above, the definition of m_ν counts each cycle ν times, so the expected number of unique cycles is

$$\overline{m}_\nu^u = \frac{\tilde{\alpha}\tilde{q}}{\alpha q} \frac{e^{\tau\nu}}{\nu}.$$

The number of cycles is related to the eigenspectrum of the adjacency matrix through Eq. (1). Therefore, from Eq. (13) we have that the expected value of the ν -th moment of the distribution of eigenvalues is

$$\overline{\langle \lambda^\nu \rangle} = \frac{1}{N} \sum_i \overline{\lambda_i}^\nu = \frac{1}{N} \frac{\tilde{\alpha}\tilde{q}}{\alpha q} e^{\tau\nu}. \quad (15)$$

We can use this relation to obtain the expected value of the leading eigenvalue by considering the limit of large ν :

$$\lim_{\nu \rightarrow +\infty} \left(\sum_i \overline{\lambda_i}^\nu \right)^{\frac{1}{\nu}} = \overline{\lambda_1} = e^\tau. \quad (16)$$

Note that the expressions for the configuration ensemble can be recovered by taking $q = \tilde{q}$, which, according to Eq. (14), implies $\tau = \ln \alpha$. Thus, the leading eigenvalue in the directed configuration ensemble is $\tilde{\lambda}_1 = \alpha = \langle k^{in} k^{out} \rangle / \langle k \rangle$. If the graph were symmetric ($k_i^{in} = k_i^{out} = k_i, \forall i$), we would have $\tilde{\lambda}_1 = \langle k^2 \rangle / \langle k \rangle$; while for the Erdős-Rényi ensemble we obtain $\lambda_1^{ER} = 1 + \langle k \rangle$. These particular cases are in agreement with previous mean-field results for these ensembles [15, 16]. The expected distribution of eigenvalues is entirely defined by its full set of moments, as given by Eq. (15). For instance, the moment-generating function for graphs with given τ is

$$M_\lambda(t) = \sum_{\nu=0}^{\infty} \frac{t^\nu}{\nu!} \overline{\langle \lambda^\nu \rangle} = \left(1 - \frac{1}{N} \frac{\tilde{\alpha}\tilde{q}}{\alpha q} \right) + \frac{1}{N} \frac{\tilde{\alpha}\tilde{q}}{\alpha q} \exp(te^\tau). \quad (17)$$

Empirical networks. We have obtained the adjacency matrices of 62 directed networks from various sources. Several details of each, including references, are listed in Tables S1–S4 of Supplemental Material. There are three broad classes of biological network in our dataset: food webs, gene regulatory networks, and metabolic networks; we also include a neural network, and several man-made networks: two of international trade, a P2P file-sharing network, and a network of concatenated English words. In all cases we have removed self-edges if present, mainly because these are not reported for many of the networks, and the nature of self-interaction is often different from that occurring between elements. However, in Supplemental Material we also analyse the same networks while conserving self-edges when reported, and the results do not differ significantly. Figure 1 displays the leading eigenvalues, λ_1 , against τ for the 62 networks, with different classes of network identified by the symbols, as indicated. The coherence ensemble expected value given by Eq. (14), shown with

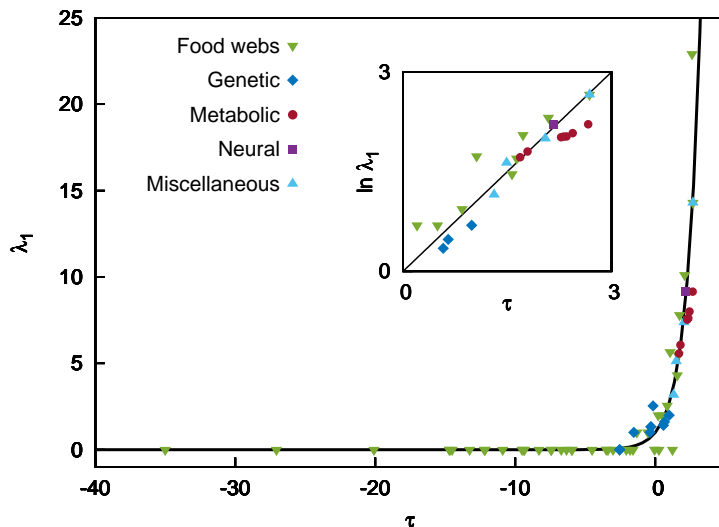


Figure 1. Leading eigenvalues λ_1 of several directed networks, against τ as given by Eq. (14); symbols indicate food webs (green down-pointing triangles), gene regulatory networks (dark blue diamonds), metabolic networks (Burgundy circles), a neural network (purple square), and other miscellaneous networks (light blue up-pointing triangles). Line: Expected leading eigenvalue $\bar{\lambda}_1$ in the coherence ensemble, as given by Eq. (16). Inset: Semi-log version of the positive quadrant of the main panel (Pearson's correlation coefficient: $r^2 = 0.87$). For these results, self-edges were removed from the networks; a similar figure in which self-edges are included can be found in SM. Details for each network, including references, are listed in the tables of SM.

a line, provides a good estimate of almost all the empirical values. The inset shows the positive quadrant on a semi-log scale. Of the 62 networks in our dataset, 36 have $\tau < 0$ and 26 have $\tau > 0$. The mean values of λ_1 for these are, respectively, $\lambda_1(\tau < 0) = 0.22 \pm 0.54$ and $\lambda_1(\tau > 0) = 6.1 \pm 7.4$. In other words, the two regimes are separated by an order of magnitude in the leading eigenvalue.

Table 1 shows the mean and standard deviation of several magnitudes for the three main classes of biological network in our dataset. The first three rows are for the ratios of measured values to the basal mean-field ensemble expectations. The food webs are significantly coherent ($q/\bar{q} < 1$) and have slightly lower mean trophic levels than the expectation ($\langle s \rangle/\bar{s} \lesssim 1$). The gene regulatory networks have coherence and mean trophic levels which are very close to their expected values. Meanwhile, the metabolic networks are significantly incoherent ($q/\bar{q} > 1$) and have mean trophic levels which are higher than expected ($\langle s \rangle/\bar{s} > 1$). The measured values of α are in all cases slightly higher than the expectation, but in the cases of food webs and gene regulatory networks, the difference is not significant. However, the metabolic networks display significant positive correlations between in- and out-degrees ($\alpha/\bar{\alpha} > 1$). The fourth row shows

the proportion of networks in each class which have negative τ . For the food webs and gene regulatory networks, it is 74% and 63%, respectively, while the metabolic networks are all in the positive τ regime. This leads to average leading eigenvalues, shown in the fifth row, which are much greater for metabolic networks than for food webs or gene regulatory networks.

	Food webs	Genetic	Metabolic
q/\tilde{q}	0.44 ± 0.17	0.99 ± 0.05	1.81 ± 0.11
$\langle s \rangle/\tilde{s}$	0.88 ± 0.18	1.00 ± 0.001	2.05 ± 0.01
$\alpha/\tilde{\alpha}$	1.02 ± 0.23	1.19 ± 0.34	3.98 ± 1.04
$\tau < 0$	31/42	5/8	0/7
λ_1	1.54 ± 4.09	1.36 ± 0.75	7.36 ± 1.20

Table 1. Mean values and standard deviation of the ratios q/\tilde{q} , $\langle s \rangle/\tilde{s}$ and $\alpha/\tilde{\alpha}$, and of the leading eigenvalue λ_1 , for three classes of biological network; and fraction of these networks to have $\tau < 0$ of the total in our dataset.

Figure 2 shows three example networks, one from each class: the Ythan Estuary food web [17], the *Chlamydia pneumoniae* metabolic network [18], and the gene regulatory network of *E. coli* [19]. The height of each node on the vertical axis is proportional to its trophic level, and this visualisation is enough to show that the trophic structures of these systems can be highly informative. Note, in particular, that a network can display significant trophic coherence (the Ythan Estuary food web has $q/\tilde{q} = 0.15$) without all its nodes falling into clearly defined trophic levels, while it is also possible to be almost bipartite, as in the case of *E. coli*'s gene regulatory network, yet be less significantly coherent as compared to the random expectation ($q/\tilde{q} = 0.88$). These examples show that in order to predict the extent of feedback in a given system, one must compute τ .

Directed acyclic graphs. Let us consider the probability that a graph randomly chosen from the coherence ensemble will have exactly m_ν cycles of length ν . We shall assume that each path is an independent random event with two possible outcomes: with probability \bar{c}_ν it is a cycle, while with $1 - \bar{c}_\nu$ it is not. The number of cycles m_ν will therefore be binomially distributed:

$$p(m_\nu) = \binom{\tilde{n}_\nu}{m_\nu} \bar{c}_\nu^{m_\nu} (1 - \bar{c}_\nu)^{\tilde{n}_\nu - m_\nu}. \quad (18)$$

We can use this distribution to obtain the probability that a network from the coherence ensemble would have no directed cycles of length greater or equal to n :

$$P_n = \prod_{\nu=n}^{\infty} p(m_\nu = 0).$$

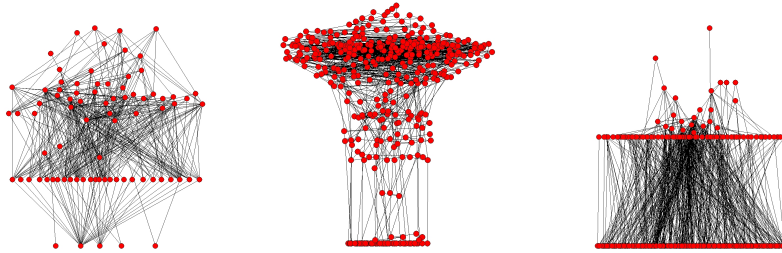


Figure 2. Examples of three kinds of network, plotted in such a way that the height of each node on the vertical axis is proportional to its trophic level (the scale used for each network is different because of the disparity in mean trophic level). Left: Ythan Estuary food web [17], which is significantly more trophically coherent than the random expectation ($q/\tilde{q} = 0.147$) and has no significant k^{in} - k^{out} correlations ($\alpha/\tilde{\alpha} = 0.935$); it is in the negative τ regime: $\tau = -1.319$. Centre: *Chlamydia pneumoniae* metabolic network [18], which is significantly less trophically coherent than the random expectation ($q/\tilde{q} = 1.621$), and has positive k^{in} - k^{out} correlations ($\alpha/\tilde{\alpha} = 2.550$); it is in the positive τ regime: $\tau = 1.686$. Right: Gene regulatory network of *E. coli* [19], which is only slightly more trophically coherent than the random expectation ($q/\tilde{q} = 0.878$) and has no significant k^{in} - k^{out} correlations ($\alpha/\tilde{\alpha} = 0.938$); it is in the negative τ regime: $\tau = -2.543$. Details for each network, including references, are listed in the tables of SM.

For instance, the probability that a network drawn randomly from this ensemble would be acyclic is

$$P_{acyclic} = \prod_{\nu=2}^{\infty} p(m_{\nu} = 0) = \prod_{\nu=2}^{\infty} \left\{ 1 - \frac{\tilde{\alpha}\tilde{q}}{Lq} \exp \left[\frac{\nu}{2} \left(\frac{1}{\tilde{q}^2} - \frac{1}{q^2} \right) \right] \right\}^{L\alpha^{\nu-1}}.$$

Taking logarithms and considering graphs with sufficiently negative τ that we can use the approximation $\ln(1-x) \simeq -x$, we have

$$\ln P_{acyclic} \simeq -\frac{\tilde{\alpha}\tilde{q}}{\alpha q} \sum_{\nu=1}^{\infty} e^{\tau\nu};$$

and, after performing the sum and some algebra,

$$P_{acyclic} \simeq \exp \left[-\frac{\tilde{\alpha}\tilde{q}}{\alpha q} \frac{1}{(e^{-\tau} - 1)} \right]. \quad (19)$$

Therefore, as $\tau \rightarrow -\infty$, networks are almost always acyclic. We note that these sums include small values of ν for which results are only approximate unless the distribution of trophic differences, $p(x)$, is Gaussian.

Figure 3 is a scatter plot of our set of empirical networks according to the terms in Eq. (14): $1/q^2 - 1/\tilde{q}^2$ and $\ln \alpha$. Each network is represented with a either a triangle or a circle depending on whether it has cycles or not, respectively. The curve $\tau = 0$ separates the two regimes, and it is clear that while

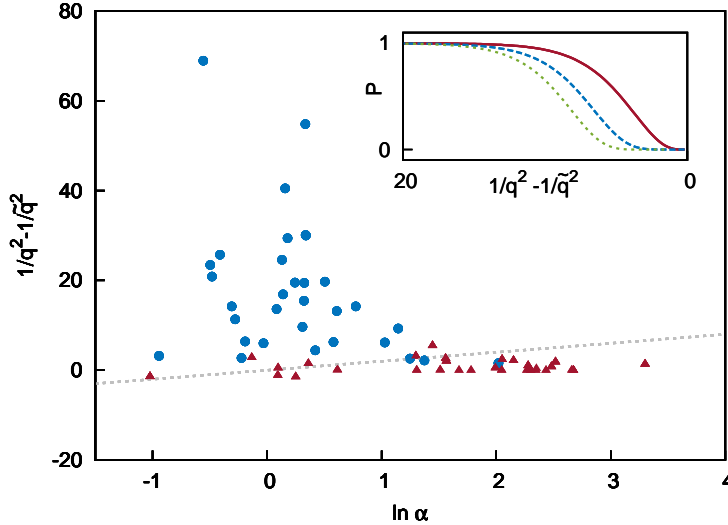


Figure 3. Scatter plot of several networks according to $1/q^2 - 1/\tilde{q}^2$ and $\ln \alpha$, the two terms in Eq. (14). Blue circles: network with no cycles. Burgundy triangles: networks with at least one cycle. The $\tau = 0$ line is shown with a dashed line (the negative τ regime falls above the line). Details for each network, including references, are listed in the tables of SM. Inset: Probabilities of networks in the coherence ensemble being acyclic, according to Eq. (19), as a function of $1/q^2 - 1/\tilde{q}^2$. Solid line: $L/L_B = 10$ and $\alpha = 1$; dashed line: $L/L_B = 100$ and $\alpha = 1$; dotted line: $L/L_B = 100$ and $\alpha = 2$.

most of the networks in the positive τ regime have cycles (the exceptions being two food webs), as one moves into the negative τ regime all the examples are acyclic. The inset shows the probability of a network randomly drawn from the coherence ensemble being acyclic, as given by Eq. (19) and indicated in the caption.

Discussion

We have shown that a directed network can belong to either of two regimes characterised by fundamentally different cycle structures, depending on the sign of a single parameter, τ , which depends on the trophic coherence and on the correlations between in- and out-degrees, as given by Eq. (14). Since the expected number of cycles of length ν is proportional to $e^{\tau\nu}$, positive τ implies an exponentially growing number of cycles with length, while for negative τ the probability of finding cycles is vanishing. This, in turn, has a crucial effect on the spectral properties of graphs: in particular, the expected value of the leading eigenvalue of the adjacency matrix is $\bar{\lambda}_1 = e^\tau$. A corollary is that graphs drawn randomly from the negative τ regime have a high probability of being directed acyclic graphs, the main requisite for qualitative stability [1].

Our results provide expected values for what we have called the coherence ensemble – the set of directed graphs with given degree sequence and trophic coherence – and do not, therefore, place bounds on the possible values a given network can exhibit. However, analysis of a set of empirical networks of various kinds shows that in most cases these expected values are very good approximations to the ones measured, suggesting that the coherence ensemble may be an appropriate null-model to use in many cases. We should note also that we have focused on binary networks (those with adjacency matrices of only ones and zeros). While some of the results could be extended to weighted networks in a straightforward way, it is not obvious how concepts such as trophic coherence should be understood when a distinction between excitatory and inhibitory interactions is made. We leave such questions for future work.

The fact that many biological networks have non-trivially few feedback loops has recently been attributed to considerations of robustness [10], stability [9], and to an “inherent directionality” [20]. Our results are compatible with the latter, since network directionality would ensue from trophic coherence (that is, since the distribution of differences $p(x)$ is centred at 1 and has variance q^2 , the expected number of edges with $x < 0$ is $L \int_{-\infty}^0 p(x) dx$, a monotonically increasing function of q). However, a suppression of cycles does not in itself induce trophic coherence, as can be easily seen in the case of the “cascade model” [21]. In this network assembly model, there is an imposed hierarchy of nodes; directed edges are placed at random with the only constraint that the out-node must be below the in-node in the hierarchy, thus emulating the situation in many food webs where predators tend to be larger than their prey. Such networks are by construction acyclic, yet they do not exhibit significant trophic coherence [11]. On the other hand, our analysis indicates that any network formation processes which tended to induce a certain trophic coherence would confer the properties of a low or negative τ on a system, without necessarily being the result of an optimization for low feedback. For example, in ecosystems many features of species, such as body size and metabolic rate, are related to trophic levels. Since predators often specialise in consuming prey with specific characteristics, they naturally focus on relatively narrow trophic ranges, with the consequence that food webs are highly coherent [11].

This relation between node function and trophic level may be at play in other systems too. For instance, we obtained the network of concatenated words included in the dataset by assigning each word in the children’s book *Green Eggs and Ham*, by Dr Seuss, to a node, and placing an edge $a_{ij} = 1$ whenever word i preceded word j in a sentence [22]. This network is no more coherent than the random expectation ($q/\bar{q} = 1.01$), yet there is clearly information in the trophic structure: the mean trophic level of common nouns is $s_{noun} = 1.4 \pm 1.2$, while that of verbs is $s_{verb} = 7.0 \pm 2.7$. (This word network is shown in Fig. S3 of Supplemental Material, with a colour code for syntactic function.) This shows that in networks where node function is encoded in trophic levels, any mechanism whereby edges tended to occur between nodes with specific functions might develop non-trivial coherence (or incoherence). More broadly, it also suggests that the trophic structure of directed networks may provide insights into their function and dynamics. Classifying nodes by trophic level, as has long been standard in ecology, might also tell us something about the functions of, say, genes, metabolites, neurons, economic agents, or words in unknown or

encrypted languages. In view of these considerations, we believe that further exploration of the trophic structure of networks, and its relation to function and dynamics, will prove a fruitful avenue for learning about complex systems.

Acknowledgements

Many thanks to M.A. Muñoz and V. Domínguez-García for a fruitful collaboration from which some of these ideas sprouted. We are grateful to I. Johnston, M. Ibáñez Berganza and J. Klaise for useful discussions. Thanks also to L. Albergante, J. Dunne, U. Jacob, R.M. Thompson, C.R. Townsend, U. Alon, M.E.J. Newman, W. de Nooy, and J. Leskovec for providing data or making them available online (see SM.)

References

- [1] R. M. May, “Qualitative stability in model ecosystems,” *Ecology*, vol. 54, pp. 638–41, 1973.
- [2] A. Arenas, A. Díaz-Guilera, J. Kurths, Y. Moreno, and C. Zhou, “Synchronization in complex networks,” *Phys. Rep.*, vol. 469, pp. 93–153, 2008.
- [3] A. E. Brouwer and W. H. Haemers, *Spectra of graphs*. Springer Science & Business Media, 2011.
- [4] M. Fiedler, “Algebraic connectivity of graphs,” *Czech. Math. J.*, vol. 23, pp. 298–305, 1973.
- [5] M. E. J. Newman, “Modularity and community structure in networks,” *Proc. Natl. Acad. Sci. USA*, vol. 103, pp. 8577–8582, 2006.
- [6] B. Bollobás, C. Borgs, J. Chayes, and O. Riordan, “Percolation on dense graph sequences,” *Ann. Prob.*, vol. 38, pp. 150–183, 2010.
- [7] R. M. May, “Will a large complex system be stable,” *Nature*, vol. 238, pp. 413–14, 1972.
- [8] A. Barrat, M. Barthélemy, and A. Vespignani, *Dynamical Processes on Complex Networks*. Cambridge: Cambridge University Press, 2008.
- [9] J. J. Borrelli, “Selection against instability: stable subgraphs are most frequent in empirical food webs,” *Oikos*, 2015.
- [10] L. Albergante, J. J. Blow, and T. J. Newman, “Buffered Qualitative Stability explains the robustness and evolvability of transcriptional networks,” *eLife*, vol. 3, p. e02863, 2014.
- [11] S. Johnson, V. Domínguez-García, L. Donetti, and M. A. Muñoz, “Trophic coherence determines food-web stability,” *Proc. Natl. Acad. Sci. USA*, vol. 111, no. 50, pp. 17923–17928, 2014.
- [12] J. Klaise and S. Johnson, “From neurons to epidemics: How trophic coherence affects spreading processes,” *Chaos (in press)*; *arXiv:1603.00670*, 2016.

- [13] V. Domínguez-García, S. Johnson, and M. A. Muñoz, “Intervality and coherence in complex networks,” *Chaos (in press)*; *arXiv:1603.03767*, 2016.
- [14] H. Kim, C. I. Del Genio, K. E. Bassler, and Z. Toroczkai, “Constructing and sampling directed graphs with given degree sequences,” *New J. Phys.*, vol. 14, p. 023012, 2012.
- [15] F. Chung, L. Lu, and V. Vu, “Spectra of random graphs with given expected degrees,” *Proc. Natl. Acad. Sci. USA*, vol. 100, no. 11, pp. 6313–6318, 2003.
- [16] R. R. Nadakuditi and M. E. J. Newman, “Spectra of random graphs with arbitrary expected degrees,” *Phys. Rev. E*, vol. 87, p. 012803, Jan 2013.
- [17] M. Huxham, S. Beaney, and D. Raffaelli, “Do parasites reduce the chances of triangulation in a real food web?,” *Oikos*, vol. 76, pp. 284–300, 1996.
- [18] H. Jeong, B. Tombor, R. Albert, Z. N. Oltvai, and A.-L. Barabási, “The large-scale organization of metabolic networks,” *Nature*, vol. 407, no. 6804, pp. 651–654, 2000.
- [19] D. Thieffry, A. M. Huerta, E. Pérez-Rueda, and J. Collado-Vides, “From specific gene regulation to genomic networks: a global analysis of transcriptional regulation in escherichia coli,” *Bioessays*, vol. 20, no. 5, pp. 433–440, 1998.
- [20] V. Domínguez-García, S. Pigolotti, and M. A. Muñoz, “Inherent directionality explains the lack of feedback loops in empirical networks,” *Sci. Rep.*, vol. 4, p. 7497, 2014.
- [21] J. E. Cohen and C. M. Newman, “A stochastic theory of community food webs I. models and aggregated data,” *Proc. R. Soc. London Ser. B.*, vol. 224, pp. 421–448, 1985.
- [22] Dr Seuss, *Green Eggs and Ham*. Random House, 1960.

Supplemental Material for *Spectra and cycle structure of trophically coherent graphs*

Samuel Johnson^{1*} and Nick S. Jones²

¹Warwick Mathematics Institute, and Centre for Complexity Science,
University of Warwick, Coventry CV4 7AL, United Kingdom.

²Department of Mathematics, Imperial College London,
London SW7 2AZ, United Kingdom.

*E-mail: S.Johnson.2@warwick.ac.uk

1 Random graphs and the basal mean-field ensemble

In the main text we define the ‘basal mean-field’ network ensemble for given number of nodes N , number of basal nodes B (those with no incoming edges), number of edges L , and number of basal edges L_B (those which are connected to basal nodes). This ensemble includes all networks in which all non-basal nodes have the same proportion of edges connected to basal nodes; in other words, every non-basal node i with in-degree k_i^{in} receives $k_i^{in} L_B/L$ edges from basal nodes and $(1 - L_B/L)k_i^{in}$ from non-basal nodes. We show that the expected mean trophic level in this ensemble is

$$\tilde{s} = 1 + \left(1 - \frac{B}{N}\right) \frac{L}{L_B}, \quad (1)$$

which corresponds to Eq. (6) of the main text; and that the expected value of the incoherence parameter is

$$\tilde{q} = \sqrt{\frac{L}{L_B} - 1}, \quad (2)$$

or Eq. (8) of the main text.

Figure S1 displays the results of Monte Carlo simulations which support the conjecture that the basal mean field ensemble provides a good approximation to more general random graph ensembles as regards trophic structure. We consider a directed version of the Erdős-Rényi ensemble, in which L directed edges are distributed randomly among N nodes with the constraint that there must be B basal nodes. We also take the directed configuration ensemble of networks, which restricts both the in- and out-degrees of each node to specified values, and generate scale-free networks by drawing those values from independent distributions $p(k) \sim k^{-\gamma}$, for $k = k^{in}$ and $k = k^{out}$. The left panel of Fig. S1 shows the mean trophic level $\langle s \rangle$ obtained numerically from Erdős-Rényi networks and

scale-free networks, as described, for varying proportions of basal nodes. This is plotted against the corresponding values given by Eq. (1) in each case. Similarly, the right panel of Fig. S1 shows the incoherence parameter q against the value given by Eq. (2), for the same networks. In both cases, the results fall very close to the $f(x) = x$ line, suggesting that the trophic structure of random graphs, regardless of their degree heterogeneity, is well approximated by the basal mean-field ensemble we have defined above. This is not surprising: if the edges of a network are placed at random among the nodes – with or without constraints on the in- or out-degree sequences – the expected fraction of edges which emanate from basal nodes is the same for every non-basal node. Therefore, in the thermodynamic limit both the random graph ensembles described above (Erdős-Rényi and configuration) should be equivalent to the basal-mean field ensemble. However, for finite N , B , L and L_B (and, in particular, for small mean degree), fluctuations around these expected proportions will induce some variability in the trophic levels of non-basal nodes. It is therefore desirable to check numerically that any discrepancies between the ensembles are small for networks of the sizes and densities we are interested in. This result thus lends support to the use of basal mean-field values as a comparison point, or random expectation, against which to compare the empirical values of real networks.

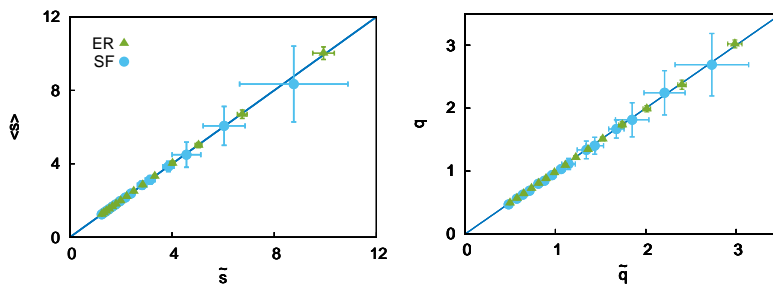


Figure S 1. Values of mean trophic level $\langle s \rangle$ (left), and incoherence parameter q (right), obtained numerically with two random graph models against the corresponding predictions for the basal mean-field ensemble, as given by Eqs. (1) and (2), respectively. The random graphs are sampled from the Erdős-Rényi ensemble (circles) with $N = 300$ and $\langle k \rangle = L/N = 10$; and from the configuration ensemble (triangles) with $N = 500$, $\langle k \rangle = L/N = 5$ and power-law degree sequences of exponent $\gamma = 3$. In both cases, the proportion of basal nodes, B/N , is varied from 10% (upper right hand corners) to 50% (lower left hand corners).

2 Networks with self-cycles

In the main text we ignore self-edges (cycles of length one) in those networks which exhibit them; this is mainly because self-edges are not reported in all networks, the nature of self-interaction often being considered fundamentally different to that of inter-element interaction. However, for completeness we also

compute the values of the largest eigenvalue λ_1 , and of the parameter τ , defined as

$$\tau = \ln \alpha + \frac{1}{2\bar{q}^2} - \frac{1}{2q^2}, \quad (3)$$

when self-edges are allowed, and display these values in Fig. S2 (compare with Fig. 2 of the main text). We can observe that the good fit to the expression

$$\bar{\lambda}_1 = e^\tau \quad (4)$$

– Eq. (16) of the main text, where $\bar{\lambda}_1$ is the randomly expected value of λ_1 – is not significantly affected by the inclusion of self-edges. The main difference is that several of the food webs which have $\lambda_1 = 0$ when self-edges are excluded now have $\lambda_1 = 1$, as a result of cannibalism.

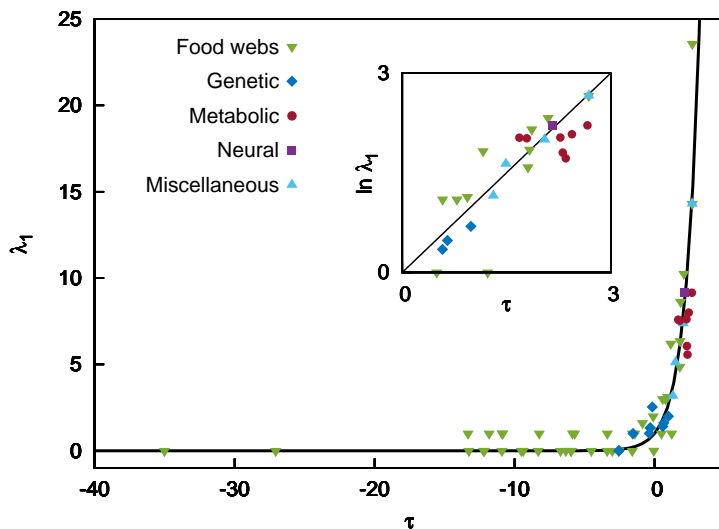


Figure S 2. Leading eigenvalues λ_1 of several directed networks when self-edges are not excluded, against τ as given by Eq. (3); symbols indicate food webs (green down-pointing triangles), gene regulatory networks (dark blue diamonds), metabolic networks (Burgundy circles), a neural network (purple square), and other miscellaneous networks (light blue up-pointing triangles). Line: Expected leading eigenvalue $\bar{\lambda}_1$ in the coherence ensemble, as given by Eq. (4). Inset: Semi-log version of the positive quadrant of the main panel (Pearson's correlation coefficient: $r^2 = 0.80$). Compare with Fig. 2 of the main text, for which self-edges are excluded. Details for each network, including references, are listed in Tables S1, S2, S3 and S4 (though note that in these tables self-edges are excluded).

3 Network data

In the main text we assess the validity of our analytical results through comparisons with a set of empirical directed networks. Most of these are available online, but a few of them were shared with us in private correspondence. Below we list the most relevant details for each of these networks. Table 1 is for 42 food webs, Table S2 lists eight gene regulatory networks, and Table S3 contains information on seven metabolic networks. Table S4 is for six networks of various other kinds: the neural network of *C. elegans*, a P2P file sharing network, two networks of trade between nations (one of basic manufactured good and the other of minerals) and one of concatenated English words in the book *Green Eggs and Ham*, by Dr. Seuss; the last of these was obtained from the original text for this work [1].

For each network, we list the number of nodes N , the number of basal nodes B and the mean degree $\langle k \rangle$; the incoherence parameter q and its ratio to the expected value \tilde{q} (low ratios mean more coherent networks than randomly expected); the mean trophic level $\langle s \rangle$ and the k^{in} - k^{out} correlation parameter α , both normalised by their expected values; the key parameter τ , whose sign determines whether a network is in the high or low feedback regimes (see main text); the largest eigenvalue, λ_1 , of the adjacency matrix; and, finally, references to the sources of the data.

Food web	N	B	$\langle k \rangle$	q	q/\tilde{q}	$\langle s \rangle/\bar{s}$	$\alpha/\bar{\alpha}$	τ	λ_1	Ref.
Benguela Current	29	2	6.76	0.69	0.15	0.17	0.69	0.50	2	[2]
Berwick Stream	77	35	3.12	0.18	0.53	1.05	1.06	-12.21	0	[3, 4, 5]
Blackrock Stream	86	49	4.36	0.19	0.57	1.02	1.27	-9.51	0	[3, 4, 5]
Bridge Brook Lake	25	8	5.08	0.53	0.36	0.68	0.72	-0.53	1	[6]
Broad Stream	94	53	6.00	0.14	0.49	1.05	1.20	-20.10	0	[3, 4, 5]
Canton Creek	102	54	6.82	0.15	0.57	1.01	1.22	-14.52	0	[7]
Caribbean Reef	50	3	10.70	0.94	0.33	0.36	0.96	1.73	7.80	[8]
Cayman Islands	242	10	15.55	0.77	0.24	0.30	0.51	1.22	0	[9]
Catlins Stream	48	14	2.29	0.20	0.41	0.98	1.00	-10.90	0	[3, 4, 5]
Chesapeake Bay	31	5	2.16	0.45	0.33	0.73	0.90	-1.81	0	[10, 11]
Coachella Valley	29	3	8.38	1.20	0.48	0.47	0.91	1.63	5.48	[12]
Coweeta 1	58	28	2.17	0.30	0.64	1.00	1.08	-3.39	0	[3, 4, 5]
Coweeta 17	71	38	2.08	0.24	0.60	1.00	1.25	-5.94	0	[3, 4, 5]
Dempsters (Au)	83	46	4.99	0.21	0.57	1.08	1.02	-7.42	0	[3, 4, 5]
Dempsters (Sp)	93	50	5.78	0.13	0.38	1.07	1.11	-27.07	0	[3, 4, 5]
Dempsters (Su)	107	50	9.02	0.27	0.57	1.05	1.04	-3.51	0.01	[3, 4, 5]
El Verde Rainforest	155	28	9.72	1.01	0.45	0.49	1.21	2.09	10.12	[13]
German Stream	84	48	4.19	0.20	0.47	1.02	1.10	-9.35	0	[3, 4, 5]
Healy Stream	96	47	6.60	0.22	0.53	1.03	1.12	-6.34	0	[3, 4, 5]
Kyeburn Stream	98	58	6.42	0.18	0.62	1.02	1.18	-9.39	0	[3, 4, 5]
LilKyeburn Stream	78	42	4.81	0.23	0.53	1.01	1.10	-5.97	0	[3, 4, 5]
Little Rock Lake	92	12	10.7	0.67	0.22	0.25	0.77	1.06	5.66	[14]
Lough Hyne	349	49	14.62	0.60	0.37	0.59	0.63	0.85	2.56	[15, 16]
Martins Stream	105	48	3.27	0.32	0.58	0.99	1.26	-2.56	0	[3, 4, 5]
Narrowdale Stream	71	28	2.17	0.23	0.50	0.98	1.17	-7.45	0	[3, 4, 5]
NE Shelf	79	2	17.44	0.73	0.13	0.10	0.71	1.57	4.32	[17]

North Col Stream	78	25	3.09	0.28	0.52	0.98	1.36	-4.52	0	[3, 4, 5]
Powder Stream	78	32	3.44	0.22	0.47	0.99	1.12	-8.32	0	[3, 4, 5]
Scotch Broom	85	1	2.58	0.40	0.14	0.30	1.20	-2.08	0	[18]
Skipwith Pond	25	1	7.56	0.61	0.15	0.16	0.64	0.20	2	[19]
St Marks Estuary	48	6	4.54	0.63	0.37	0.63	1.02	0.26	0	[20]
St Martin Island	42	6	4.88	0.59	0.32	0.54	0.79	-0.05	0.01	[21]
Stony Stream	109	61	7.59	0.15	0.55	1.03	1.16	-14.66	0	[22]
Stony Stream 2	112	63	7.41	0.15	0.55	1.04	1.18	-14.72	0	[3, 4, 5]
Sutton (Au)	80	49	4.19	0.15	0.66	1.08	1.28	-13.27	0	[3, 4, 5]
Sutton (Sp)	74	50	5.28	0.10	0.56	1.11	1.15	-35.01	0	[3, 4, 5]
Sutton (Su)	87	63	4.87	0.28	0.89	1.19	0.52	-1.59	0	[3, 4, 5]
Troy Stream	77	40	2.35	0.19	0.37	1.01	1.14	-12.16	0	[3, 4, 5]
UK Grassland	61	8	1.59	0.40	0.18	0.42	0.63	-3.03	0	[23]
Venlaw Stream	66	30	2.83	0.23	0.54	1.06	1.35	-6.72	0	[3, 4, 5]
Weddel Sea	483	61	31.71	0.72	0.55	0.75	1.17	2.63	22.91	[24]
Ythan Estuary	82	5	4.77	0.42	0.15	0.28	0.93	-1.32	1	[25]

Table S 1. Details of 42 food webs used in the main text. Columns are for number of nodes N , number of basal nodes B , mean degree $\langle k \rangle$, and incoherence parameter q ; ratios of q , mean trophic level $\langle s \rangle$, and correlation parameter α to their expected values in the basal mean field ensemble; parameter τ , leading eigenvalue λ_1 , and references to the data sources. Many of the data are available online at:

https://www.nceas.ucsb.edu/interactionweb/html/thomps_towns.html

Gene regulatory network	N	B	$\langle k \rangle$	q	q/\tilde{q}	$\langle s \rangle/\tilde{s}$	$\alpha/\tilde{\alpha}$	τ	λ_1	Ref.
Human (healthy)	4071	4004	2.08	0.08	0.99	1.00	0.99	-1.54	1	[26, 27]
Human (cancer)	4049	3967	2.89	0.08	1.00	1.00	1.07	-0.16	2.54	[26, 27]
<i>E. coli</i> (Salgado)	1470	1316	1.98	0.23	1.03	1.00	1.21	0.65	1.62	[28, 27]
<i>E. coli</i> (Thieffry)	418	312	1.24	0.27	0.88	1.01	0.94	-2.54	0	[29, 30]
<i>S. cerevisiae</i> (Harbison)	2933	2764	2.10	0.17	0.98	1.00	1.29	-0.38	1	[31, 27]
<i>S. cerevisiae</i> (Costanzo)	688	557	1.57	0.25	1.04	1.00	0.81	-0.31	1.32	[32, 30]
<i>P. aeruginosa</i>	691	606	1.43	0.30	1.00	1.03	1.94	0.58	1.41	[33, 27]
<i>M. tuberculosis</i>	1624	1542	1.95	0.17	1.02	1.00	1.24	0.99	2.00	[34, 27]

Table S 2. Details of eight gene regulatory networks (GRN) used in the main text. The *E. coli* (Salgado) and Yeast (Harbison) are available online at:

<http://wvs.weizmann.ac.il/mcb/UriAlon/download/collection-complex-networks>. The others were shared with us by Luca Albergante, and some of them can be obtained from various websites: <http://regulondb.ccg.unam.mx/> (*E. coli*, Salgado); http://younglab.wi.mit.edu/regulatory_code (Yeast, Harbison); <http://www.genome.gov/ENCODE/> (Human, both the non-cancer GM12878 cell line and the K562 leukaemia cell line). Columns as in Table S1.

Metabolic network	N	B	$\langle k \rangle$	q	q/\bar{q}	$\langle s \rangle/\bar{s}$	$\alpha/\bar{\alpha}$	τ	λ_1	Ref.
<i>A. fulgidus</i>	1267	36	2.38	13.79	1.88	2.06	4.34	2.35	7.62	[35]
<i>M. thermoautotrophicum</i>	1111	30	2.43	12.17	1.77	1.90	4.08	2.31	7.59	[35]
<i>M. jannaschii</i>	1081	32	2.40	12.47	1.86	1.98	4.00	2.27	7.53	[35]
<i>C. pneumoniae</i>	386	20	2.05	8.98	1.62	1.71	2.55	1.69	5.57	[35]
<i>C. trachomatis</i>	446	19	2.11	11.77	1.95	2.02	2.77	1.79	6.07	[35]
<i>S. cerevisiae</i> (yeast)	1510	43	2.54	14.61	1.73	1.82	5.54	2.66	9.15	[35]
<i>C. elegans</i>	1172	40	2.44	13.29	1.86	2.04	4.60	2.44	8.00	[35]

Table S 3. Details of seven metabolic networks used in the main text, downloaded from <http://www3.nd.edu/~networks/resources.htm>. Columns as in Table S1.

Network (miscellaneous)	N	B	$\langle k \rangle$	q	q/\bar{q}	$\langle s \rangle/\bar{s}$	$\alpha/\bar{\alpha}$	τ	λ_1	Ref.
Neural (<i>C. elegans</i>)	297	3	7.90	1.49	0.42	0.39	1.42	2.17	9.15	[36, 37]
P2P (Gnutella 2008)	6301	3836	3.30	0.98	0.98	1.00	1.07	1.49	5.12	[38, 39]
Trade (manufactured goods)	24	2	12.92	4.24	1.14	1.14	1.10	2.68	14.3	[40]
Trade (minerals)	24	3	5.63	4.04	1.02	0.97	1.28	2.05	7.38	[40]
Words	50	16	2.02	2.04	1.01	1.16	1.55	1.31	3.17	[1]

Table S 4. Details of six other networks used in the main text. The network of words was obtained for this work from *Green Eggs and Ham* [1], and is available upon request from s.johnson.2@warwick.ac.uk. The other data can be found on various websites:
<http://www-personal.umich.edu/~mejn/netdata/> (neural network);
<https://snap.stanford.edu/data/p2p-Gnutella08.html> (P2P network);
and <http://vlado.fmf.uni-lj.si/pub/networks/data/esna/metalWT.htm> (trade networks). Columns as in Table S1

4 Green Eggs and Ham words network

We obtained the network of concatenated words from Dr Seuss’s masterpiece *Green Eggs and Ham* in the following way [1]. Every node in the text was assigned a node, and a directed edge $a_{ij} = 1$ was placed whenever word i preceded word j in a sentence. Figure S3 displays this network in such a way that the height of each node on the y-axis is proportional to its trophic level. Note that the arrows we have placed between nodes in this visualisation are from the preceding word to the succeeding one, so that one can obtain sentences (some of them grammatically correct) by following the arrows. We have used colours to indicate syntactic function, as described in the caption. There is clearly a relation between the trophic level of a word in this network and its function. Might a similar relation hold for other kinds of system, such as gene regulatory networks?

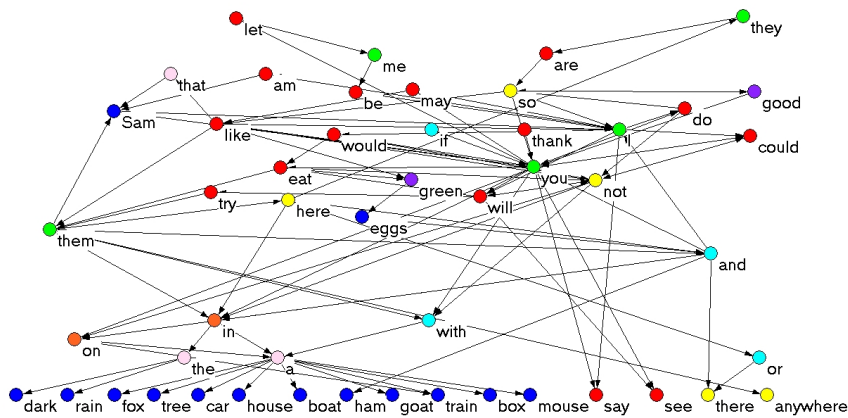


Figure S 3. Network of concatenated words from *Green Eggs and Ham*, by Dr Seuss [1]. The height of each word is proportional to its trophic level. Colours indicate syntactic function; from lowest to highest mean trophic level: nouns (blue), prepositions and conjunctions (cyan), determiners (pink), adverbs (yellow), pronouns (green), verbs (red), and adjectives (purple). When a word has more than one function, the one most common in the text is used.

References

- [1] Dr Seuss, *Green Eggs and Ham*. Random House, 1960.
- [2] P. Yodzis, “Local trophodynamics and the interaction of marine mammals and fisheries in the benguela ecosystem,” *Journal of Animal Ecology*, vol. 67, no. 4, pp. 635–658, 1998.
- [3] R. M. Thompson and C. R. Townsend, “Impacts on stream food webs of native and exotic forest: An intercontinental comparison,” *Ecology*, vol. 84, pp. 145–161, 2003.
- [4] R. M. T. and C. R. Townsend, “Energy availability, spatial heterogeneity and ecosystem size predict food-web structure in stream,” *Oikos*, vol. 108, p. 137–148, 2005.
- [5] Townsend, Thompson, McIntosh, Kilroy, Edwards, and Scarsbrook, “Disturbance, resource supply, and food-web architecture in streams,” *Ecology Letters*, vol. 1, no. 3, pp. 200–209, 1998.
- [6] K. Havens, “Scale and structure in natural food webs,” *Science*, vol. 257, no. 5073, pp. 1107–1109, 1992.
- [7] Townsend, Thompson, McIntosh, Kilroy, Edwards, and Scarsbrook, “Disturbance, resource supply, and food-web architecture in streams,” *Ecology Letters*, vol. 1, no. 3, pp. 200–209, 1998.

- [8] S. Opitz, “Trophic interactions in Caribbean coral reefs,” *ICLARM Tech. Rep.*, vol. 43, p. 341, 1996.
- [9] J. Bascompte, C. Melián, and E. Sala, “Interaction strength combinations and the overfishing of a marine food web,” *Proceedings of the National Academy of Sciences of the United States of America*, vol. 102, no. 15, pp. 5443–5447, 2005.
- [10] R. E. Ulanowicz and D. Baird, “Nutrient controls on ecosystem dynamics: the chesapeake mesohaline community,” *Journal of Marine Systems*, vol. 19, no. 1–3, pp. 159 – 172, 1999.
- [11] L. G. Abarca-Arenas and R. E. Ulanowicz, “The effects of taxonomic aggregation on network analysis,” *Ecological Modelling*, vol. 149, no. 3, pp. 285 – 296, 2002.
- [12] G. Polis, “Complex trophic interactions in deserts: an empirical critique of food-web theory,” *Am. Nat.*, vol. 138, pp. 123–125, 1991.
- [13] R. B. Waide and W. B. R. (eds.), *The Food Web of a Tropical Rainforest*. Chicago: University of Chicago Press, 1996.
- [14] N. D. Martinez, “Artifacts or attributes? Effects of resolution on the Little Rock Lake food web,” *Ecol. Monogr.*, vol. 61, pp. 367–392, 1991.
- [15] J. Riede, U. Brose, B. Ebenman, U. Jacob, R. Thompson, C. Townsend, and T. Jonsson, “Stepping in Elton’s footprints: a general scaling model for body masses and trophic levels across ecosystems,” *Ecology Letters*, vol. 14, pp. 169–178, 2011.
- [16] A. Eklöf, U. Jacob, J. Kopp, J. Bosch, R. Castro-Urgal, B. Dalsgaard, N. Chacoff, C. deSassi, M. Galetti, P. Guimaraes, S. Lomáscolo, A. Martín González, M. Pizo, R. Rader, A. Rodrigo, J. Tylianakis, D. Vazquez, and S. Allesina, “The dimensionality of ecological networks,” *Ecology Letters*, vol. 16, pp. 577–583, 2013.
- [17] J. Link, “Does food web theory work for marine ecosystems?,” *Mar. Ecol. Prog. Ser.*, vol. 230, pp. 1–9, 2002.
- [18] J. Memmott, N. D. Martinez, and J. E. Cohen, “Predators, parasitoids and pathogens: species richness, trophic generality and body sizes in a natural food web,” *J. Anim. Ecol.*, vol. 69, pp. 1–15, 2000.
- [19] P. H. Warren, “Spatial and temporal variation in the structure of a fresh-water food web,” *Oikos*, vol. 55, pp. 299–311, 1989.
- [20] R. R. Christian and J. J. Luczkovich, “Organizing and understanding a winter’s Seagrass foodweb network through effective trophic levels,” *Ecol. Model.*, vol. 117, pp. 99–124, 1999.
- [21] L. Goldwasser and J. A. Roughgarden, “Construction of a large Caribbean food web,” *Ecology*, vol. 74, pp. 1216–1233, 1993.

- [22] Townsend, Thompson, McIntosh, Kilroy, Edwards, and Scarsbrook, “Disturbance, resource supply, and food-web architecture in streams,” *Ecology Letters*, vol. 1, no. 3, pp. 200–209, 1998.
- [23] N. D. Martinez, B. A. Hawkins, H. A. Dawah, and B. P. Feifarek, “Effects of sampling effort on characterization of food-web structure,” *Ecology*, vol. 80, p. 1044–1055, 1999.
- [24] U. Jacob, A. Thierry, U. Brose, W. Arntz, S. Berg, T. Brey, I. Fetzer, T. Jonsson, K. Mintenbeck, C. Möllmann, O. Petchey, J. Riede, and J. Dunne, “The role of body size in complex food webs,” *Advances in Ecological Research*, vol. 45, pp. 181–223, 2011.
- [25] M. Huxham, S. Beaney, and D. Raffaelli, “Do parasites reduce the chances of triangulation in a real food web?,” *Oikos*, vol. 76, pp. 284–300, 1996.
- [26] M. B. Gerstein, A. Kundaje, M. Hariharan, S. G. Landt, K.-K. Yan, C. Cheng, X. J. Mu, E. Khurana, J. Rozowsky, R. Alexander, *et al.*, “Architecture of the human regulatory network derived from encode data,” *Nature*, vol. 489, no. 7414, pp. 91–100, 2012.
- [27] L. Albergante, J. J. Blow, and T. J. Newman, “Buffered Qualitative Stability explains the robustness and evolvability of transcriptional networks,” *eLife*, vol. 3, p. e02863, 2014.
- [28] H. Salgado, M. Peralta-Gil, S. Gama-Castro, A. Santos-Zavaleta, L. Muñiz-Rascado, J. S. García-Sotelo, V. Weiss, H. Solano-Lira, I. Martínez-Flores, A. Medina-Rivera, *et al.*, “Regulondb v8. 0: omics data sets, evolutionary conservation, regulatory phrases, cross-validated gold standards and more,” *Nucleic Acids Research*, vol. 41, no. D1, pp. D203–D213, 2013.
- [29] D. Thieffry, A. M. Huerta, E. Pérez-Rueda, and J. Collado-Vides, “From specific gene regulation to genomic networks: a global analysis of transcriptional regulation in escherichia coli,” *Bioessays*, vol. 20, no. 5, pp. 433–440, 1998.
- [30] R. Milo, S. Itzkovitz, N. Kashtan, R. Levitt, S. Shen-Orr, I. Ayzenshtat, M. Sheffer, and U. Alon, “Superfamilies of evolved and designed networks,” *Science*, vol. 303, no. 5663, pp. 1538–1542, 2004.
- [31] C. T. Harbison, D. B. Gordon, T. I. Lee, N. J. Rinaldi, K. D. Macisaac, T. W. Danford, N. M. Hannett, J.-B. Tagne, D. B. Reynolds, J. Yoo, *et al.*, “Transcriptional regulatory code of a eukaryotic genome,” *Nature*, vol. 431, no. 7004, pp. 99–104, 2004.
- [32] M. C. Costanzo, M. E. Crawford, J. E. Hirschman, J. E. Kranz, P. Olsen, L. S. Robertson, M. S. Skrzypek, B. R. Braun, K. L. Hopkins, P. Kondu, *et al.*, “YpdTM, pombepdTM and wormpdTM: model organism volumes of the bioknowledgeTM library, an integrated resource for protein information,” *Nucleic Acids Research*, vol. 29, no. 1, pp. 75–79, 2001.
- [33] E. Galán-Vásquez, B. Luna, and A. Martínez-Antonio, “The regulatory network of pseudomonas aeruginosa,” *Microb Inform Exp*, vol. 1, no. 1, pp. 3–3, 2011.

- [34] J. Sanz, J. Navarro, A. Arbués, C. Martín, P. C. Marijuán, and Y. Moreno, “The transcriptional regulatory network of mycobacterium tuberculosis,” *PloS one*, vol. 6, no. 7, p. e22178, 2011.
- [35] H. Jeong, B. Tombor, R. Albert, Z. N. Oltvai, and A.-L. Barabási, “The large-scale organization of metabolic networks,” *Nature*, vol. 407, no. 6804, pp. 651–654, 2000.
- [36] J. G. White, E. Southgate, J. N. Thompson, and S. Brenner, “The structure of the nervous system of the nematode caenorhabditis elegans,” *Phil. Trans. R. Soc. London*, vol. 314, pp. 1–340, 1986.
- [37] D. J. Watts and S. H. Strogatz, “Collective dynamics of ‘small-world’ networks,” *Nature*, vol. 393, pp. 440–442, 1998.
- [38] J. Leskovec, J. Kleinberg, and C. Faloutsos, “Graph evolution: Densification and shrinking diameters,” *ACM Transactions on Knowledge Discovery from Data*, vol. 1, 2007.
- [39] M. Ripeanu, I. Foster, and A. Iamnitchi, “Mapping the gnutella network: Properties of large-scale peer-to-peer systems and implications for system design,” *IEEE Internet Computing Journal*, 2002.
- [40] W. de Nooy, A. Mrvar, and V. Batagelj, *Exploratory Social Network Analysis with Pajek*. Cambridge: Cambridge University Press, 2004.